LBL-36666
UC-406

Lawrence Berkeley Laboratory
UNIVERSITY OF CALIFORNIA

Accelerator & Fusion
Research Division

To be published as a chapter in *Ion Beam Therapy*, U. Linz, Ed.,
Chapman & Hall, London, England, 1995

Radiation Detectors

W.T. Chu

January 1995

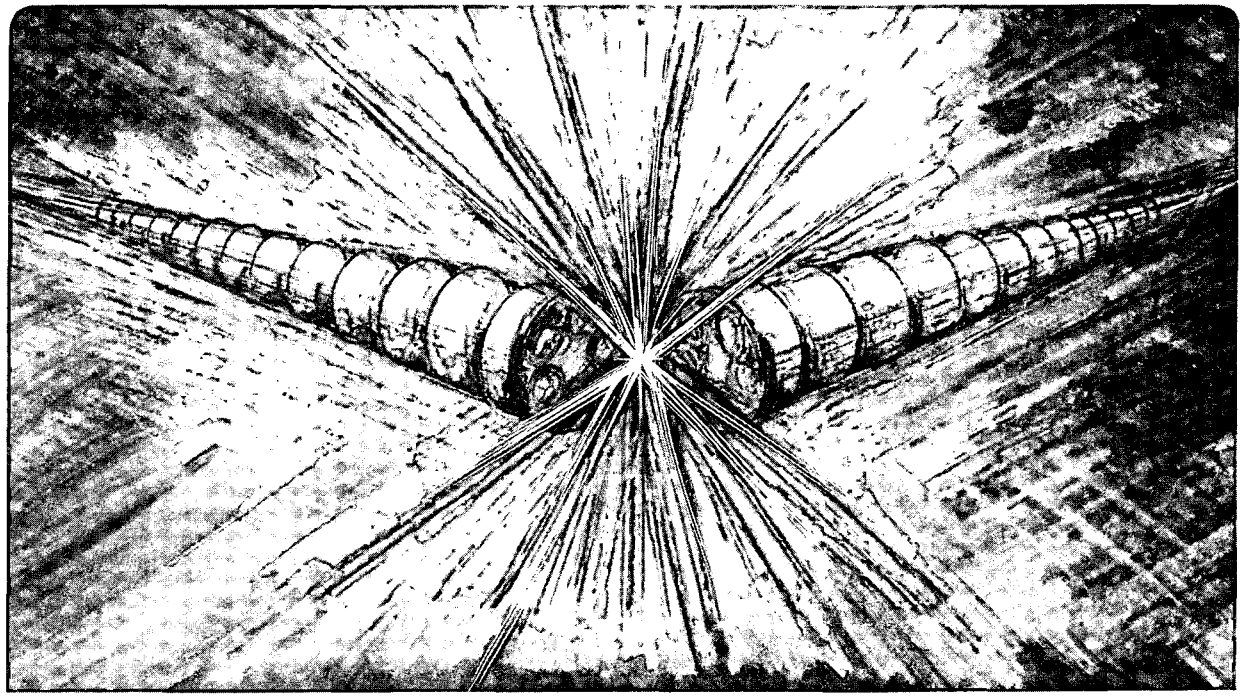

Prepared for the U.S. Department of Energy under Contract Number DE-AC03-76SF00098

DISCLAIMER

LBL-36666
UC-406

RADIATION DETECTORS*

W.T. Chu

Lawrence Berkeley Laboratory
University of California
Berekeley, CA 94720

January 1995

To be published in Ion Beam Therapy (Ed. Ute Linz),
Chapman & Hall, pp. 234-245 (in press, to be published in August 1995.

* This work was supported by the Director, Office of Energy Research, Energy Research Laboratory Technology Transfer Program of the U.S. Department of Energy under Contract No. DE-AC03-76SF00098.

To be published in *Ion Beam Therapy* (ed. U. Linz), Chapman & Hall, pp. 234-245 (in press, to be published in August 1995).

Radiation Detectors

W. T. Chu, Lawrence Berkeley Laboratory
University of California, Berkeley, CA 94720, USA

Introduction.

Ion-beam treatments of humans with radiation require accurate, reliable, and safe methods for controlling the ion beams. An accurate delivery of the prescribed dose is essential for achieving the desired cure and preventing an overdose of radiation. In principle, if the beam is properly tuned and the beam delivery is functioning correctly, then one absolute or properly-calibrated radiation detector is sufficient for measuring the delivered dose. In practice, however, depending on the complexity of the beam delivery system, several detectors, with possibly many sub-divided detection elements, are needed for achieving the required level of accuracy and safety.

Radiation detectors that are clinically used perform three main functions: 1) real-time measurement of the delivered dose to the patient in order to terminate the irradiation at the prescribed dose, 2) measurement of the spatial distribution of the radiation delivered in order to ensure that the patient prescription is satisfied, and 3) measurement of radiation field parameters at selected points along the beam line for controlling the beam-delivery system. The last function is required as ion beams from the accelerator undergo range changes, spatial deflections, and nuclear interactions before reaching the patient. From a utilitarian point of view, these radiation detectors may be categorized according to their applications, such as: detectors for absolute calibration measurements, dose detectors whose signals are proportional to absorbed dose, radiation detectors that can be used to measure dose after being calibrated for a particular type of radiation, and specialized detectors which measure properties of individual particles, e.g., lineal energy transfer (LET) of the projectile particle. Basic dosimetric detectors are usually used in an integrating mode, but their time response must meet the rapidity requirements of termination of the irradiation procedures. Fast detector

response is also called for in controlling dynamic beam delivery or measurement of the time structure of extracted beams from an accelerator.

In order to measure the dose delivered to the patient precisely, the dose detectors must measure a quantity proportional to the dose imparted to the patient. They must achieve this without significantly perturbing the radiation field, i.e., without degrading the radiation quality. For light-ion beams which contain many particle species with a wide range of LET values due to fragmentation of the projectile particles, the dose detectors must measure the dose independent of the LET distribution in the beam. Large radiation detectors with fine spatial resolution are important for comparing the prescribed and delivered radiation distributions over the entire treatment area. A required dose accuracy for clinical purposes of ±2.5%, measured over a large dynamic range (~10^6), adds to the complexity of monitoring the radiation.

Many of the radiation detectors described in this chapter have been developed for single particle detection in nuclear physics measurements. Several have been used in the dosimetry of conventional radiation (photons and electrons). How these detectors are used in ion-beam therapy is the subject of this chapter. The radiation detectors used in ion-beam therapy were described in a recent review article (1), therefore, in this chapter new materials are described more extensively while others are briefly discussed for completeness.

Ionization Chambers.

At many ion-beam therapy facilities, ionization chambers (2) are often used as the primary dose measuring devices because of their accuracy, reliability and ease of operation. When an ion beam traverses an ionization chamber, it produces the ionization in the gas, which is proportional to the energy loss by the beam, which is in turn approximately proportional to the dose absorbed by the detector. This dose can then be related to the absorbed dose in another medium, such as human tissue, by the ratio of the stopping power of the gas to that of the medium. The ionization charge, Q(coulombs), produced by the beam passing through such a chamber is proportional to the absorbed dose, D(Gy), which is given by the Bragg-Gray equation (3): $Q=D\rho V/W$, where $\rho(kg/m^3)$ is the mass density, $V(m^3)$ is the volume, and W(eV) is the ionization

energy needed to produce an ion pair. Hence, D can be obtained by measuring Q if the value of W is known.

Therefore, the accuracy of the dose measured using ionization chambers is limited by the accuracy of the W-value. The accurate knowledge of W value is particularly important if intercomparisons of clinical results from various centers are to be made. Recently there have been many studies for accurate determination of the W values (4-7). Based on the results of these studies, the best value of W for proton beams is considered to be 34.5±0.7 eV (8). The W value varies for different particle types and velocities. This becomes a critical issue when using heavier ion beams because the beams generally contain a mixture of particles (fragments) at various energies produced in the beam modifying devices. For heavier ions the W value of 33.7 eV is used (9).

Transmission ionization chamber.

The most common type of ionization chambers used in ion-beam therapy is the transmission type. A typical chamber consists of two parallel planes with an electric field applied between them for collection of ionization charges (10). The effective mass of the chamber per unit area must be reduced so that the chamber has little effect on scattering or fragmenting the beam particles. A typical chamber is schematically depicted in Fig. 1, which is composed of the support body, gas windows, signal and high-voltage planes, and the electrical and gas connections. Thin nonconducting (e.g., Kapton) foils make up beam entrance and exit windows enclosing a gas volume. Additional foils define a pair of parallel planes and create a known ionization volume. One foil is connected to a high voltage source and the other, a collecting foil, is connected to appropriate electronics for measuring the ionization charge. The properties of the gas used in these chambers determine ionization yield and recombination probability of the charge carriers before their collection.

Gases such as nitrogen, air, tissue-equivalent gas, and argon have been regularly used in ionization chambers. Nitrogen gas or air are most commonly used because their ionization potential, W-value, and stopping power ratio of gas to tissue(S_m) are better known and their saturation levels are acceptable at beam intensities used for ion-beam therapy. Air is also practical because its temperature and pressure variations can be easily measured and corrected for

and the humidity of the air has a negligible effect on the detector response. At high beam intensities where saturation effects become important, an inert gas which does not form negative ions, such as Ar or He, can be used. For example, recombination effects for Ne ions would not be expected up to ~200 Gy/sec for Ar gas as compared to ~20 Gy/sec with air. For higher yields Xe gas can be used with a lower W-value and a higher density. For fast response times He gas has been used because of its higher ion drift velocity.

Thimble ionization chambers.

Because a direct measurement of dose in the patient is not practical, the dosimeters are calibrated against a reference ionization detector, usually a thimble ionization chamber, placed inside a phantom target volume in conditions similar to an actual treatment. Thimble ionization chambers are spherical or cylindrical chambers made from conductive plastic with a center stem for charge collection. The plastic walls are typically a few mm thick and the sensitive volumes are usually between 0.1 cm^3 and 1.0 cm^3 or greater. Smaller chambers afford better spatial resolution, but are less sensitive. Such detectors serve as practical calibration devices after they are calibrated against a national standard, such as the one at the National Institute of Standards and Technology in the US. These chambers are primarily used with air or a tissue-equivalent gas as the ionization medium.

Segmented ionization chambers.

When radiation fields used are larger than a few centimeters across, it is necessary to pay close attention to the field uniformity. An ionization chamber with segmented collection elements located as close as possible to the patient is best suited in providing the desired on-line information. Segmentation of the collecting planes provides a means of obtaining information on spatial dose distribution. The number of elements can range from several to a few thousands and their geometric arrangement can be tailored to suit the beam spreading system. For example, a collecting element segmented into a set of concentric rings can measure beam profiles with cylindrical symmetry (11). Other geometric arrangements can be constructed to measure the beam profiles that lack cylindrical symmetries. Examples are: the 19 hexagonal elements (5 cm across) arranged in honeycomb fashion (Fig. 2) and the 144-

element (a 12 x 12 array of 2.5 cm x 2.5 cm areas) chamber both used at LBL (10), and the 400-element (a 20 x 20 array of 1 cm x 1 cm areas) chamber at Loma Linda University Medical Center, Loma Linda, California (12). In these chambers, the signals are extracted through thin traces located on the opposite side of the foil from the collection elements. Holes drilled through the foil, which are then plated through, allow connections between the elements and traces as schematically shown in Fig. 2. This method avoids collection of charge on these traces by placing them away from any electric field.

The 3600-element chamber.

An ionization chamber with a sensitive area of 30 cm x 30 cm with 0.5 cm spatial resolution was built at LBL by dividing the collecting plane into a 60 x 60 array of 5 mm x 5 mm areas (13). The detector was specifically designed to minimize its impact on the beam and the space it occupies in the beam line; its physical thickness is 5 cm and the water-equivalent thickness 2 mm. The main difficulty to be overcome was the crowded condition of bringing out signal leads from the 3600 collection areas. This problem was solved by placing the signal leads in four different planes of laminated material as in the multilayer construction technique developed for printed circuit technology. As a result, the spacings between the leads are made as large as 0.2 mm.

Charge integrators.

Energetic ions traversing an ionization chamber produce a charge output proportional to the deposited dose. Because the clinical beams from an accelerator have temporal structures, measuring the dose means measuring the total charge as an integral of a fluctuating current. The electronics for these devices are generally some form of charge integrator with a response time fast enough for control purposes.

A form of charge integrator that is particularly well suited to ion-beam therapy applications is the one which issues a pulse for every fixed increment of input charge (e.g., 10 pC). A standard circuit for this purpose is the charge balancing current integrator or recycling integrator (14). When used with digital electronics these circuits measure the dose with the advantages of a large dynamic range, exceptional linearity, and excellent noise immunity.

Typical radiation doses used for ion-beam therapy range from ~1 mGy to ~10 Gy. As an illustration, an ionization chamber using nitrogen gas at atmospheric pressure and room temperature with a 1.0 cm^3 volume exposed to such doses produces between 35 pC to 0.35 μC. Accounting for the variation in volumes that are used in an ionization chamber requires the current integrator to be able to measure as little as 10 pC and as large as 3.5 μC. The rate at which this dose can be delivered can vary from 10^{-3} to 1 Gy/sec and even higher instantaneous dose rates. The electronics may saturate at these high dose rates. As saturation leads to an inaccurate dose measurement, some means of detecting a saturation condition must be provided.

Secondary Emission Monitors (SEMs).

A typical SEM consists of a set of parallel foils (e.g., 6-μm thick aluminum foils separated by 3 mm) in a vacuum enclosure. The foils alternate between collection foils and bias foils. The more foils that are used, the greater is the signal. The number of secondary electrons produced by traversing ions depends on the energy deposited in the layer, called the escape zone. The work function of the material and the condition of the surface determine the thickness of this escape zone. Electron production scales linearly with foil thickness up to the point where electrons do not escape the foil. Good vacuum in the chamber is important for keeping the foil surfaces free of absorbed material which can affect the secondary electron emission. Pressure below 1 mP reduces the ionization of the residual gas to an acceptable level; however, the better the vacuum the more consistent the performance. A vacuum of 1 μP is routinely used for the purpose of beam-line monitoring. A bias voltage of approximately –50 V is applied to the bias foils to ensure nearly complete collection of the electrons which have energies less than 25 eV.

Dose measuring accuracy of an SEM can be better than 1% and the long term stability of its output is excellent. A calibration of the SEM can be done against a calibrated ionization chamber or by using the foil activation technique, a calorimeter, or a Faraday cup.

As mentioned above, at high dose rate saturation in ionization chambers can be a major problem in their use as dose-detecting devices. SEMs can serve as alternative detectors to ionization chambers. Saturation in SEMs has not been

seen in electron-beam current densities of up to tens of mA/cm^2, making their use ideal in situations where there is a concern about ionization chamber saturation. The SEM outputs are linear until space charge effects become important, which has been estimated to be above ~10^9 Gy/sec. Another advantage of a SEM detector is its fast response time, which is determined by the travel time of the electrons rather than the slower migration time of ions in an ionization chamber. Responses in the nanosecond time scale are possible. Their major disadvantage is the low yield of secondary electrons per primary particle compared with ionization chambers, that limits their use for low beam particle fluxes.

Wire Chambers.

In the simplest form, a wire chamber consists of two planes of evenly spaced parallel wires separated by a given distance, with the intervening volume filled with gas. One wire plane is used as the signal plane, and the other as the high voltage plane. The high voltage plane can also be a solid foil conductor instead of a plane of parallel wires. While the common application of wire chambers in particle physics is to detect traversing particles on a particle-by-particle basis, in ion-beam therapy applications wire chambers are more often used as integrating devices that integrate spatially along a wire as well as temporally during an irradiation procedure. Typical clinical ion-beam intensities are between 0.1 pA and 0.1 mA .

Wire chambers are typically operated in a proportional mode where a multiplication of the initial ionization occurs, but can be operated in an ionization mode where the gain is unity. In the former mode, multiplication of the initial ionization occurs when the ionized electrons, accelerated by the strong potential gradient around a wire, cause further ionization. The gain is dependent on the type and pressure of the gas, the wire spacing, and the high voltage. By decreasing the wire spacings, increased spatial resolution can be achieved at the price of decreased gain due to the decrease in potential gradient around the wires. Wire spacing as coarse as 6 mm and as fine as 0.2 mm are practical. Gold coated beryllium/copper wires of 50 μm diameter are often used because of their longevity and mechanical stability in the beam. Common gases used in such devices are air, argon, or gas mixtures such as 10% argon

and 90% CO_2. Atmospheric pressure is a convenient gas pressure; however, lower as well as higher pressures have been used. The principles of construction and operations of wire chambers have been discussed widely (15).

Two planes of sense wires placed orthogonally can show the horizontal and vertical projections of the beam profile. The centroid and the width of the beam can be computed in each plane for beam-tuning purposes. Monitoring beam profiles is important for efficiently transporting the ion beams and obtaining the correct dose distributions with the beam delivery system. Typically a wire chamber is positioned upstream of the beam delivery system and a second wire chamber is located downstream of the delivery system, near the patient. The active area of the second chamber is typically large to accommodate the large radiation fields.

MEDUSA.

A multi-wire, multi-plane wire chamber, called the Medical Dose Uniformity Sampler (MEDUSA), was developed at LBL to reconstruct the two-dimensional dose profile of a beam (16). It has 16 wire planes, each of which has 64 wires separated by 4 mm. Each plane samples the beam profile projected into the particular wire direction, which is offset by 11.25 degrees (180 degrees divided into 16 equal angles) from adjacent planes. Based on the 16 projected profile data sets, MEDUSA reconstructs the 2-dimensional dose profile within a circular area of 256-mm diameter. The reconstruction of the two dimensional image relies on the 'filtered back projection' algorithm.

Diodes and Diode Arrays.

The usefulness of diodes as dose detectors derives from their small size (17). Measuring dose distributions with fine spatial resolution is difficult with ionization chambers, but simple with diodes which intrinsically have small active areas. As a solid, they absorb a lot more dose in a small volume. Speaking generally, there are two disparate applications of diodes in a typical ion-beam therapy facility: efficient mapping of large dose fields, where the feasibility of a diode array is paramount, and mapping of very small dose fields (e.g., for eye treatments), where ionization chambers may be too large to serve. A calibration of the diode must be done before use since they suffer radiation

damage over extended exposure. They are, however, excellent for relative measurements over short time periods. Arrays of diodes have successfully been used for measuring profiles of radiation fields and Bragg ionization curves (18).

Junction diodes, connected to an electrometer which keeps the voltage across the diode nearly equal to zero, exhibit a current (in the 'reverse' direction) nearly proportional to dose rate over a wide range (19). There is extensive literature on this subject; however, most of it is about photon and electron beam applications (20). Nearly any diode will work; power rectifiers, small-signal diodes, microwave diodes, LEDs and photodiodes have all been used. Their advantages are small size, low cost, ruggedness and simplicity of use (no polarizing voltage). Their disadvantages include sensitivity to electrometer voltage burden, decline of output with accumulated dose, and (fairly small) temperature and dose-rate effects.

Commercial diodes for electronics are N-type. P-type diodes built specially for dosimetry are available. They exhibit less radiation damage and smaller dose-rate effect (20), but their cost almost rules them out for large arrays.

The associated electrometer is usually an integrator, to measure total charge produced in a monitored exposure. Diodes place a special demand on the electrometer, and their use will be frustrating unless this is taken into account: the voltage burden (voltage appearing at the integrator input during normal operation) is critically important, which is not the case with either an ionization chamber or a Faraday cup. This voltage, appearing across the effective resistance of the diode, causes a drift current which will vary with time and temperature unless the electrometer amplifier is carefully chosen. Many popular commercial electrometers are inadequate in this regard but it is not difficult to find an inexpensive opamp (e.g., the Texas Instruments TLC27L2) which is suitable (21). Unfortunately this leaves the potential user (especially of diode arrays) with an in-house construction project. The design for 64 channel integrator has been developed and tested at the Harvard Cyclotron Laboratory (HCL), and available on request.

Otherwise, the use of diode arrays is straightforward. The array of diodes should feed an array of integrators which is scanned, digitized and read out

using some standard scheme, e.g., RS-232 or CAMAC. Each channel should be read out before and after the exposure so that the difference can be taken. Because the degradation of sensitivity with integrated dose is initially larger, it helps to pre-irradiate the diodes to, say, 1000 Gy. Even so, in lengthy experiments one should calibrate the diodes before and after the run and keep track of the dose so that final corrections can be made. Diode sensitivities (pC/cGy), after pre-irradiation, have a wide range: e.g., ≈140 for a 1N4004 (1-A rectifier), ≈100 for Hamamatsu S2164 photodiode, ≈10 for a typical small-signal diode, and ≈1 for one element of and ELB-1001HDA 10-element LED array useful in mapping very small fields. These numbers will decrease substantially over the useful life of the diode. For comparison, a 0.05 cm^3 thimble ionization chamber registers about 10 pC/cGy.

When mapping large fields of high-energy ions the diode package makes no difference, but for precise work (especially near end-of-range) the photodiode, with its thin and precisely known covering layer, is an elegant package. Of course, photodiodes and LEDs must be carefully light-proofed. Exposed conductors should be covered with coil dope or RTV sealant so that charge is not picked up from ionized air. Depending on the environment, electrostatic shielding (aluminum foil crimped to the shield of the output cable) may be needed. RG-178B/U miniature Teflon insulated cable works well in this and other low signal applications because the cable itself produces little signal when exposed to radiation or when flexed. Avoid connectors, except coaxial types, wherever they might be exposed to radiation.

The use of single diodes for precise dose measurements, though convenient, is somewhat problematic. Koehler (19) reported about 8% more output from a particular diode (long since unavailable) than from a parallel-plate ionization chamber in the Bragg-peak region, when the two were made to agree in the 'entrance' region. If a thimble chamber is used as the reference dosimeter additional geometric effects come into play, and total discrepancies of ≈15% (diode vs. thimble chamber at the Bragg peak) are found at HCL (22). At present there is a wealth of (sometimes contradictory) observations, very few published. One can only conclude that (a) there is an energy dependent problem (diodes and ionization chambers, more often than not, exhibit different Bragg curves); (b) different diodes appear to give different results, as do

different ionization chambers, and (c) the problem may lie with the diodes, the ionization chambers, or both. Energy dependence in proton beam dosimetry at the 5–10% level simply requires further study.

At HCL a dose scanner within a water phantom has been developed. A small water phantom with approximately 15 cm x 15 cm entrance window and 18 cm depth along the proton beam is supported on a 3-axis computer-controlled positioning system that can quickly and reproducibly place the tank anywhere in a therapy field. Within the tank, a 4th axis controls the depth of a detector module containing a thimble ionization chamber, an 8 x 6 array of diodes, a 'stairstep' array of diodes for depth detection, and 3 diodes for edge scanning. The system can be manually controlled either locally or remotely, or by a computer command file.

The system takes advantage of the reduced scattering of protons vis-a-vis photons to use a much smaller tank. It is only necessary to ensure that any detector within the tank is surrounded laterally by a radius R of water (or plastic) such that any beam conditions outside of R have an insignificant effect on the dose at the detector. For 160-MeV protons, R=2 cm is sufficient for most situations but R=5 cm was chosen for a wide safety margin. The weight of the resulting tank is small enough that the entire tank can be moved to position the detectors laterally after moving from a parking position out of the way of patients undergoing therapy. Deployment of the tank which remains filled with water, aligned with the beam, and connected to the necessary integrators and electrometer can be accomplished in about a minute. Quicker and more detailed scans of patient treatment beams are the result.

The detector module supports the various detectors in a dry environment, surrounded by plastic, within the water tank. An Exradin T1 tissue equivalent ionization chamber is laterally centered in the module, but with only a small amount of plastic window upstream. The chamber is connected to an electrometer (Keithley 617) about 30 m away, operated in the floating mode. An array of 48 photodiodes (Hamamatsu S2164) in 6 columns of 8 diodes with 10-mm column spacing and 8-mm row spacing are connected to a 64 channel integrator with very low input voltage burden using individual 3-m coaxial cables (RG174). The diode connections to the coaxial cable are potted in RTV

silicon and the entire module is electrically shielded with silver paint, and shielded from light by an additional coat of black paint. Specially edge mounted diodes are used for lateral scans of beams with very sharp penumbra. A stairstep of 8 diodes spanning 16 mm in depth in 2 mm steps is used to quickly measure a depth dose in a region of relatively uniform depth.

The Exradin ionization chamber is used for routine beam-line checks as well as individual patient therapy beam calibrations. The diodes are used for more detailed scans and for apertures too small to be accurately measured by the larger ionization chamber. The diodes can be re-calibrated automatically in 2 minutes by a sequence that measures the dose in the central region of a flat field using the ionization chamber and then serially brings the diodes into the same region in four groups to be calibrated. This procedure is necessitated by the inevitable radiation damage to the diodes, and must be repeated frequently only if large volume scans at high accuracy are required. Fig. 3 shows a depth scan using a row of 8 diodes with points taken every 1 mm of depth in the region of the Bragg peak. The alignment of the data points from diode to diode at the distal 50% shows that the variation in depth is about 0.1 mm of water. This regularity, together with accurate lateral diode positioning and ease of calibration, results in large data sets that display continuity over the many diodes involved in the scan.

Other Types of Radiation Detectors.

Several types of devices other than ionization chambers, SEMs, wire chambers, and diodes have been successfully used in ion-beam therapy applications. Each, as discussed below, has its special application.

Semiconductor detectors.

Aside from the use of diodes as discussed above, semiconductor detectors are used for many different purposes in ion-beam therapy applications.

Semiconductor detectors such as Si surface barrier detectors or thin Ge detectors are excellent for measuring the energy loss of a particle since they have high sensitivity, and their response is independent of the particle type and proportional to the energy deposited. A much smaller amount of energy is

required to produce an electron-hole pair compared to ~35 eV needed in a gas ionization chamber to produce an ion pair. However, they do suffer from a pulse height defect associated with large energy depositions leading to recombination of electron-hole pairs. A Ge crystal of sufficient thickness to stop an incoming particle can serve as a total energy detector. Ge detectors have excellent particle energy resolution, typically $dE/E \approx 0.1\%$, but radiation damage can lead to a degradation in their energy resolution. These detectors are used primarily for single particle detection and are not suitable for measurements at normal clinical beam intensities.

The biological damages due to high-LET radiation can not completely be simply described by the dose and average LET. The actual composition of the beam in terms of the particle types and their relative contributions to the biological damages must be determined. A particle detector system known as the BERKLET, has been developed at LBL in order to identify the particle charge, but not mass, along with its residual energy and LET (23). The system consists of a 300-μm thick Si detector followed by a 5.5-cm thick Ge detector. The two detectors, operated in coincidence, measure the dE/dx and the total energy of the particle, respectively. The total energy that can be measured in the Ge detector corresponds to a particle with an 18.7-cm penetration in water. Another application at LBL of solid-state detectors is the use of position-sensitive Si detectors to measure multiple Coulomb scattering and compared the data against several scattering formulas (24).

Scintillators.

In high-energy and nuclear physics experiments scintillators have been used extensively for single particle detection. In ion-beam therapy, they have been used primarily for beam controls because of their fast response times and large dynamic ranges of operation when used in conjunction with phototubes. Large beam currents cause radiation damages to the solid scintillators, which limit their lifetime and effect their response. A Xe gas scintillator has been used to control the beam at Loma Linda (25). Because light production in the scintillator is not simply proportional to the energy loss of the particle due to quenching, their use as a dose detector requires special calibration. Recently they have been used in conjunction with charged coupled devices (CCD

cameras) to measure the lateral uniformity of a radiation field and to measure the scintillation light as a function of depth for range verification (26).

Calorimeters.

The rise in temperature of a material from the energy deposited in it by an ion beam may be used for absolute dose measurement. Water temperature increases by $2.4 \times 10^{-4} K$ per Gray of deposited dose; but, making an accurate measurement is difficult. Calorimeters are not practical means of measuring dose for on-line clinical dosimetry, but rather serve as calibration standards.

Faraday Cups.

Faraday cups measure the number of particles by measuring the charges collected on an electrically isolated and evacuated container which stops the beam (27). When monoenergetic ions impinge upon the Faraday cup, the dose is calculated from the measured number of particles per unit area and the mass stopping power of the particle at the given energy in tissue.

Film.

Film is the most economical method for measuring spatial dose distributions with the finest spatial resolution available, yet it is not a rapid instrument. The spatial resolution achievable with film is limited by the resolution of the digitizing procedure, whose speed is in turn limited by the time required for digitization and data reduction. The darkening of the film, i.e., optical density, after exposure to an ion beam can be used to measure the dose. In retrospective studies at LBL, film is shown to provide better than ±5% absolute dose accuracy if the development conditions are closely controlled; however, few relies on film for clinical dosimetry. The optical density depends more on the particle fluence (number of particles per unit area) than the dose deposited. In other words, it depends on the LET of the particles. For this reason, film is primarily a relative dose detector and is used for measuring lateral dose distributions rather than depth-dose distributions which exhibit pronounced LET dependence.

Thermoluminescent dosimeters (TLDs).

TLDs are inorganic materials, such as LiF or CaF_2, that do not scintillate promptly, but rather trap electron-hole pairs created from the exposure to ionizing radiation. Upon heating the exposed material, the trapped electrons can escape, leading to light emission which can be detected, and related to the absorbed dose.

Chemical dosimeters.

In chemical dosimetry, radiation dose is determined by measuring the chemical change produced in an irradiated medium. The most well-known chemical dosimeter is the Fricke dosimeter, which determines the dose by measuring the ferric-ion yield from the oxidation of Fe^{+2} to Fe^{+3} by the interaction of the ionization and the ferrous ion. The measurement of optical density of the irradiated solution at a specific wavelength can be interpreted in terms of the ferric-ion density, which is in turn related to the dose.

One of the recent developments in the ion-beam dosimetry is the application of alanine compound. Radiation changes the chemical structure of alanine crystals, and the degrees of the chemical changes can be determined by analyzing the Zeeman hyperfine molecular levels through electron spin resonance (ESR). Its advantages are portability, tissue-equivalence, and minimal fading at ambient temperature which provides permanent irradiation record. Its LET dependence and reproducibility are still to be investigated (28).

Nuclear activation.

Foil activation utilizes the ion beam undergoing a nuclear reaction of a known cross-section in a foil of a known thickness. The radioactive yield can then be measured by means of its decay over time, which determines the initial beam intensity, and hence the imparted dose. For example, the reaction $^{12}C+p \rightarrow {}^{11}C+p+n$ has been used to determine absolute fluence and absorbed dose of protons for therapy. This method is used more for verification than on-line analysis.

As a variation of the above method, in vivo dosimetry for assessing the integral dose of a ion-beam irradiation have been studied by detecting the decay products of ^{11}C, ^{13}N and ^{15}O from tissue activation (29).

Solid-state nuclear track detectors.

The passage of energetic ions through most insulators forms narrow regions of radiation damages, called 'latent tracks.' In crystals, such a track may be detected by viewing with an electron microscope; and in polymers by means of special coloring of the track. A more practical method is to use plastic sheets and to etch the latent tracks selectively, which can subsequently be viewed with an optical microscope. Plastics such as CR39 have been extensively used to measure the LET distribution of heavy-ion beams (30). Measurements of an individual track left by traversing or stopping heavy charged particle in plastic detectors render information about their dE/dx, A, Z, and sometimes velocity. Recently the use of solid-state nuclear track detectors in nuclear physics has been reviewed (31), and lists of commercial sources of most commonly used material for solid-state nuclear track detectors are found in publications (32).

Microdosimetry.

Microdosimetry measurements utilize gas proportional counters to study energy losses on the microscopic scale, such as inside a cell. To understand the effects of the inherently statistical nature of the energy deposition in a cell, a detector comparable in water-equivalent size to a cell is required (33). Gas proportional counters are used with sizes and at gas pressures that replicate the energy deposition in a cell and which have enough gain for reasonable signal processing.

Concluding Remarks.

Many accurate and reliable radiation detectors have been developed and used in ion-beam therapy applications. However, there still remains important questions that must be answered for complete understandings of ion beams used in therapy. For example, the discrepancies in the Bragg curves obtained by different detectors, such as diodes and ionization chambers, should be explained. Some areas of future developments in radiation detectors are:

development of dose detectors which can provide a spatial resolution (≈ 1 mm) sufficient for reconstruction of dose distributions deposited in a patient using pencil-beam scanning, two-dimensional amorphous silicon detector arrays, new detectors such as the use of scintillating material or Fricke gels for three-dimensional dose measurements with a high spatial resolution.

Acknowledgments.

The author wishes to express his gratitude to Bernard Gottschalk and Miles Wagner of the Harvard Cyclotron Laboratory for providing unpublished materials on diode detectors for inclusion in this article. This work is supported by the Director, Office of Energy Research, Energy Research Laboratory Technology Transfer Program, of the U.S. Department of Energy under Contract No. DE-AC03-76SF00098.

References

1. Chu, W. T., Ludewigt, B. A. and Renner, T. R. Instrumentation for Treatment of Cancer Using Proton and Light-Ion Beams. Reviews of Scientific Instrument, 64, 2055-2122, 1993.

2. Boag, J. W. Ionization Chambers, in Radiation Dosimetry, Attix, F.H. and Roesch, W.C. (eds.), Academic Press, New York, 1966; pp 1-72.

3. Bragg, L. An ionization method for the absolute measurement of gamma-ray energy. Proc. Roy. Soc. Ser. A 156, 578, 1936.

4. Thomas, D. J. and Burke, M. W value measurements for protons in tissue-equivalent gas and its constituent gases. Phys. Med. Biol. 30, 1201-1213, 1985.

5. Petti, P. L., Verhey, L. and Wilson, R. A measurement of w for 150 MeV protons in nitrogen and argon. Phys. Med. Biol. 31, 1129-1138, 1986.

6. Seuntjens, J., Palmans, H., Verhaegen, F., Denis, J.-M., Vynckier, S. and Thierens, H. Water calorimetry for clinical proton beams. Presented at NPL calorimetry workshop, Teddington, UK, October, 1994.

7. Vatnitsky, S. M. and Siebers, J. V. Comparison of water calorimeter with reference ionization chamber dosimetry in high-energy photon and proton beams. Presented at NPL calorimetry workshop, Teddington, UK, October, 1994.

8. Verhey, L. Emerging international consensus on clinical proton dosimetry. Presented at the NIRS International Seminar on the Application of Heavy Ion Accelerator to Radiation Therapy of Cancer and the PTCOG XXI Meeting, Chiba, Japan, November 1994.

9. American Association of Physicists in Medicine, Protocols for Heavy Charged Particle Beam Dosimetry," A Report of Task Group 20, Radiation Therapy Committee, AAPM Report No. 16, American Institute of Physics, New York 1986.

10. Renner, T. R., Chu, W. T., Ludewigt, B. A., Nyman, M. A. and Stradtner, R. Multisegmented Ionization Chamber Dosimetry System for Light Ion Beams. Nucl. Instrum. Methods in Phys. Res. A281, 640-648, 1989.

11. Lyman, J. T., Howard, J. and Windsor, A. A. Heavy charged-particle beam monitoring with segmented ionization chambers. Med. Phys. 2, 163, 1975.

12. Coutrakon, G., Bauman, M., Lesyna, D., Miller, D., Nusbaum, J., Slater, J., Johanning, J., Miranda, J., DeLuca, P. M., Jr., Siebers, J. and Ludewigt, B. A prototype beam delivery system for the proton medical accelerator ar Loma Linda. Med. Phys. 18, 1093-1099, 1991.

13. Chu, W. T., Ludewigt, B. A., Marks, K. M., Nyman, M. A., Renner, T. R., Singh, R. P. and Stradtner, R. Three-Dimensional Conformal Therapy Using Light-Ion Beams. Proc. of the NIRS International Workshop on Heavy Charged Particle Therapy and Related Subjects , July 4-5, 1991, Chiba, Japan, 110-123, 1991.

14. Gottschalk, B. Charge-balancing current integrator with large dynamic range. Nucl. Instrum. Methods 207, 417-421, 1983.

15. Sauli, F. Principles of Operation of Multiwire Proportional and Drift Chambers, CERN 77-09, CERN European Organization for Nuclear Research, Geneva, Switzerland 3 May 1977.

16. Chu, W. T., Alonso, J. R. and Tobias, C. A. Heavy Ion Beam Studies and Imaging with a Multiplane Multiwire Proportional Chamber. IEEE Trans. Nucl. Sci. NS-28, 2198-2200, 1981.

17. Fowler, J. W. Solid State Electrical Conductivity Dosimeters, in Radiation Dosimetry, Attix, F.H. and Roesch, W.C. (eds.), Academic Press, New York, 1966; pp 241.

18. Gottschalk, B. "Calibrating dosimeter arrays," HCL Technical Report, Note 6/10/88, Harvard Cyclotron Laboratory, Cambridge, MA 1988.

19. Koehler, A. M. Dosimetry of proton beams using small diodes. Radiat. Res. Suppl. 7, 53-64, 1967.

20. Rikner, G. and Grusell, E. General specifications for silicon semiconductors for use in radiation dosimetry. Phys. Med. Biol. 32, 1109-1117, 1987 and references therein.

21. Gottschalk, B. Resetting a current integrator with the supply lines. Nucl. Instr. Meth. A297, 534-535, 1990.

22. Wagner, M. S., private communication (1994).

23. Llacer, J., Schmidt, J. B. and Tobias, C. A. Characterization of fragmented heavy-ion beams using a three-stage telescope detector: Detector configuration and instrumentation. Med. Phys. 17, 158-162, 1990.

24. Wong, M., Schimmerling, W., Phillips, M. H., Ludewigt, B. A., Landis, D. A., Walton, J. T. and Curtis, S. B. The multiple scattering of very heavy charged particles. Med. Phys. 17, 163-171, 1990.

25. Coutrakon, G., Miller, D., Kross, B. J., Anderson, D. F., DeLuca, P. and Siebers, J. A Beam Intensity Monitor for the Loma Linda cancer therapy proton accelerator. Med. Phys. 18, 817-820, 1991.

26. Coutrakon, G., Miller, D., Wong, J., Gere, L. and Binns, R. Characterization of the Loma Linda proton beam using a plastic scintillator and CCD camera readout. Med. Phys. 17, 543, 1990.

27. Vynckier, S., Meulders, J.-P., Robert, P. and Wambersie, A. The Proton Therapy Program at the Cyclotron "Cyclone" of Louvain-la-Neuve (First Dosimetric Results). J. Eur. Radioth, 5, 245-247, 1984.

28. Gall, K. Alanine ESR dosimeterrs, April 1993, presented at the PTCOG XVIII meeting, Nice, France 1993.

29. Graffman, S. and Jung, B. ^{11}C and ^{15}O induced in the mouse by 175 MeV protons. Acta Radiol. Therapy Phys. Biol. 14, 113-126, 1975.

30. Benton, E. V., Henke, R. P. and Tobias, C. A. Calibration of high-energy heavy-particle beams with plastic nuclear track detectors. Nucl. Track Detection 1, 139, 1977.

31. Tret'yakova, S. P. Solid-state nuclear track detectors and their use in experimental nuclear physics. Soviet J. of Particles & Nuclei 23, 156-186, 1992.

32. Fleischer, R. L., Price, P. B. and Walker, R. M. Nuclear Tracks in Solids: Priinciples and Applications, Berkeley, Univ. of Calif. Press 1975.

33. Kellerer, A. M. Fundamentals of Microdosimetry, in The Dosimetry of Ionizing Radiation, Krase, K.R., Bjarngard, B.E. & Attix, F.H. (eds.), Academic Press, New York, 1985; Vol. I.

To be published in *Ion Beam Therapy* (ed. U. Linz), Chapman & Hall, pp. 234-245 (in press, to be published in August 1995).

Captions of figures:

Fig. 1. A cross-section of a typical transmission ionization chamber.

Fig. 2. A schematic drawing of the LBL 19-element segmented ionization chamber. The segmented collection elements are shown in dotted lines and the signal traces in solid lines. The collecting elements and the signal traces are on the opposite sides of the insulating foil. The electric connections are made via holes in the foil which are plated through.

Fig. 3. Depth dose data from eight diodes in a vertical column taken with the Scanner/Phantom diode assembly. The data was taken for 2688 points in 10 minutes with the 48 diodes. In the plot only 448 points are displayed. The effect of a defining aperture is seen in the end scans. Dimensions are in cm. (Courtesy of M. Wagner, HCL.)

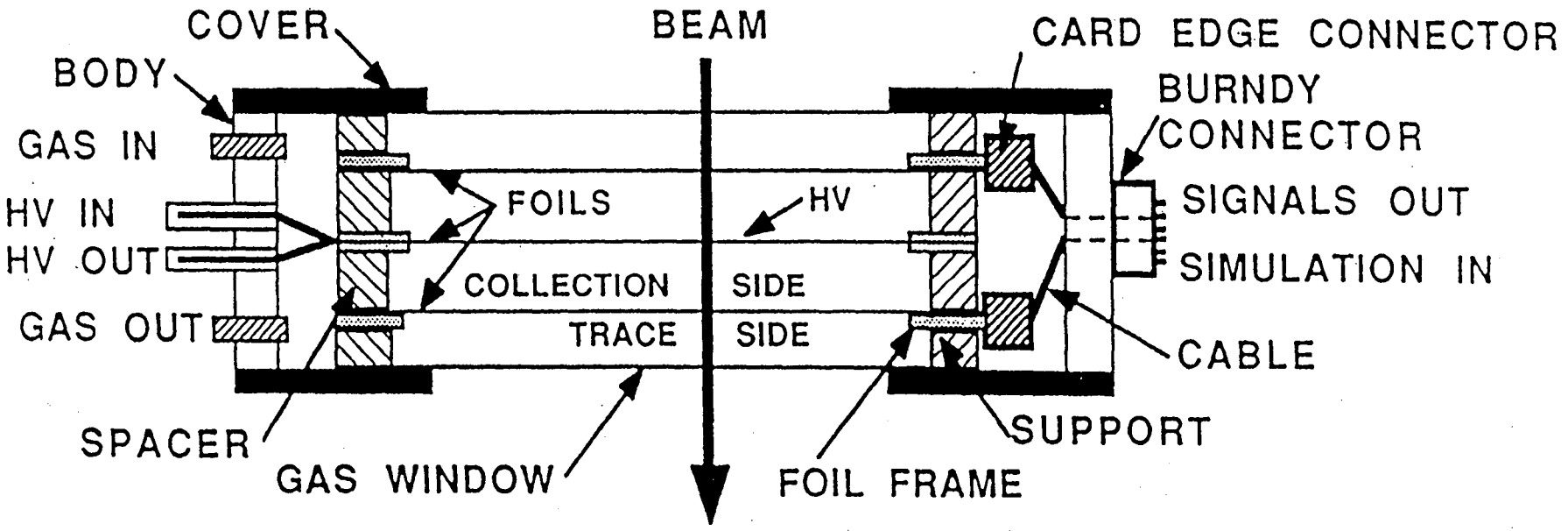
COVER
BEAM
CARD EDGE CONNECTOR
BODY
BURNDY
CONNECTOR
GAS IN
FOILS
HV
SIGNALS OUT
HV IN
HV OUT
SIMULATION IN
COLLECTION SIDE
GAS OUT
TRACE SIDE
CABLE
SPACER
GAS WINDOW
FOIL FRAME
SUPPORT

Figure 1

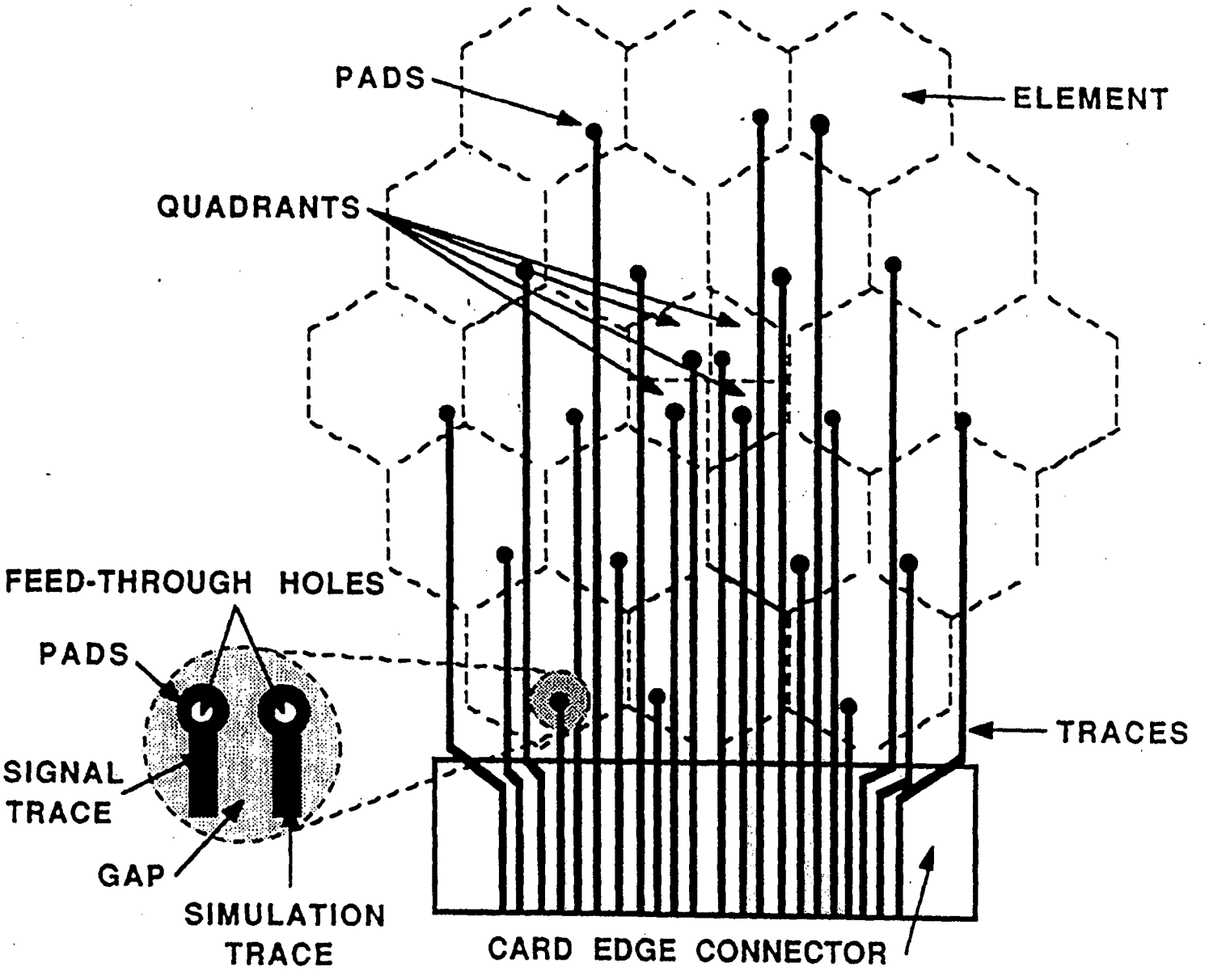
PADS
ELEMENT
QUADRANTS
FEED-THROUGH HOLES
PADS
SIGNAL TRACE
GAP
SIMULATION TRACE
TRACES
CARD EDGE CONNECTOR

Figure 2

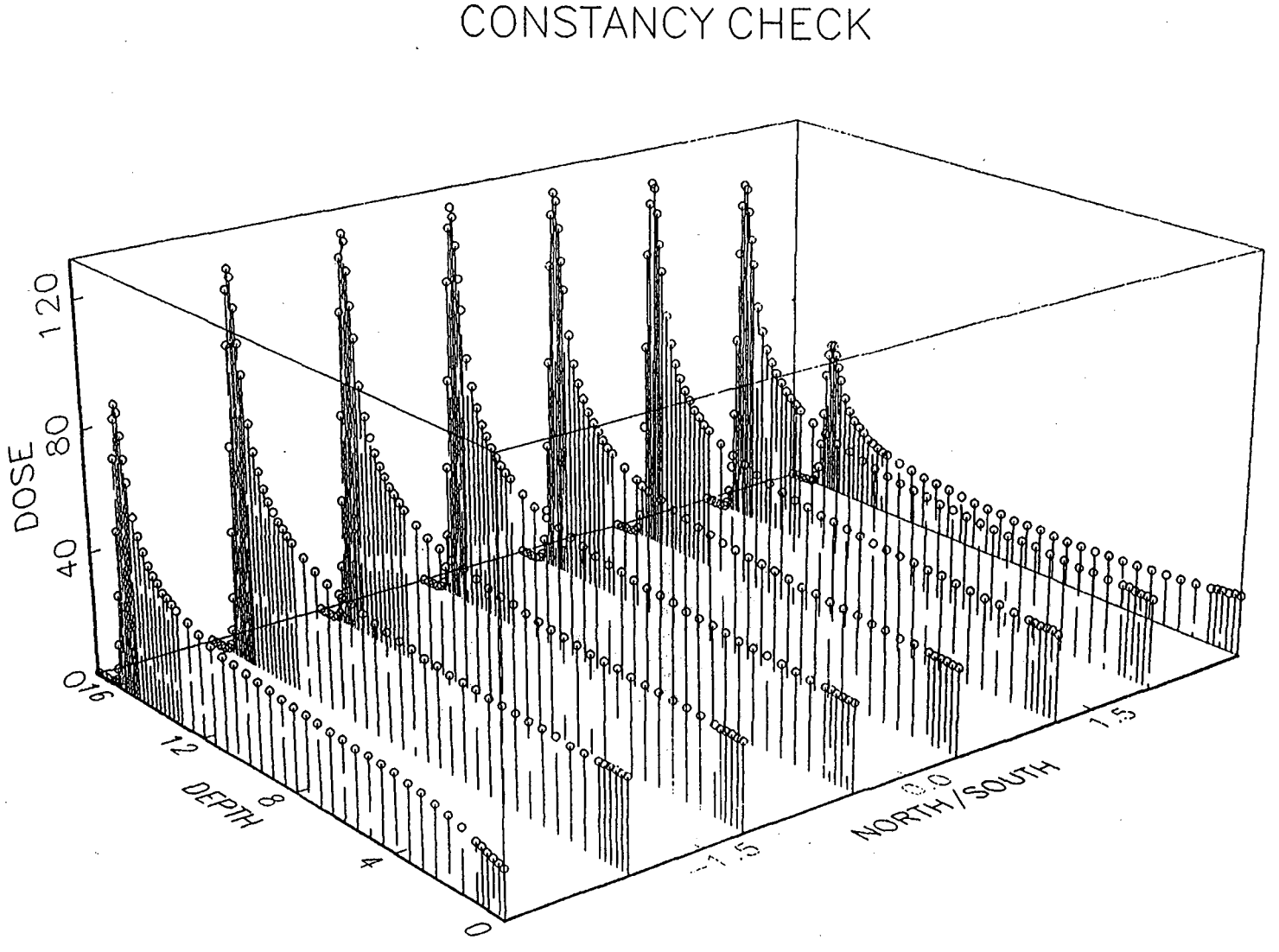
CONSTANCY CHECK
DOSE
120
80
40
0
16
12
8
4
0
DEPTH
-1.5
0.0
1.5
NORTH/SOUTH

Figure 3

LAWRENCE BERKELEY NATIONAL LABORATORY
UNIVERSITY OF CALIFORNIA
TECHNICAL & ELECTRONIC INFORMATION DEPARTMENT
BERKELEY, CALIFORNIA 94720